

Supramolecular Polymer Hydrogels for Drug-Induced Tissue Regeneration

Jing Cheng¹, Devang Amin², Jessica Latona³, Ellen Heber-Katz³, and Phillip B. Messersmith^{4}*

¹Departments of Bioengineering and Materials Science and Engineering, University of California, Berkeley, 210 Hearst Mining Building, Berkeley, CA 94720, USA.

²Department of Biomedical Engineering, Northwestern University, Evanston, Illinois 60208, USA.

³Laboratory of Regenerative Medicine, Lankenau Institute for Medical Research, Wynnewood, PA 19096, USA.

⁴Materials Sciences Division, Lawrence Berkeley National Laboratory, Berkeley, CA 94720, USA.

*Correspondence and requests for materials should be addressed to philm@berkeley.edu.

Materials and Methods

Synthesis of 1,4-dihydrophenanthroline-4-one-3-carboxylic acid (DPCA) (3). 8-aminoquinoline (14.4 g, 100 mmol) and diethyl ethoxymethylenemalonate (22.7 g, 105 mmol) were heated to 100°C for 2 h and then added diphenylether (300 mL), refluxed (250°C) for 5 h, and cooled to room temperature. The precipitate product (**2**) was separated by centrifugation, washed with 100 mL hexane twice, and then washed with 50 mL diethyl ether. After drying under vacuum overnight, the brown powder was combined with 500 mL 10% (w/v) KOH and refluxed for 2 h, cooled to 5°C, precipitated with 120 mL HCl, filtered, washed with DI water, and dried under vacuum overnight to afford crude product (**3**) as a brown powder (10 g, 41 mmol, 41%). The crude product was recrystallized in DMF before the next step.

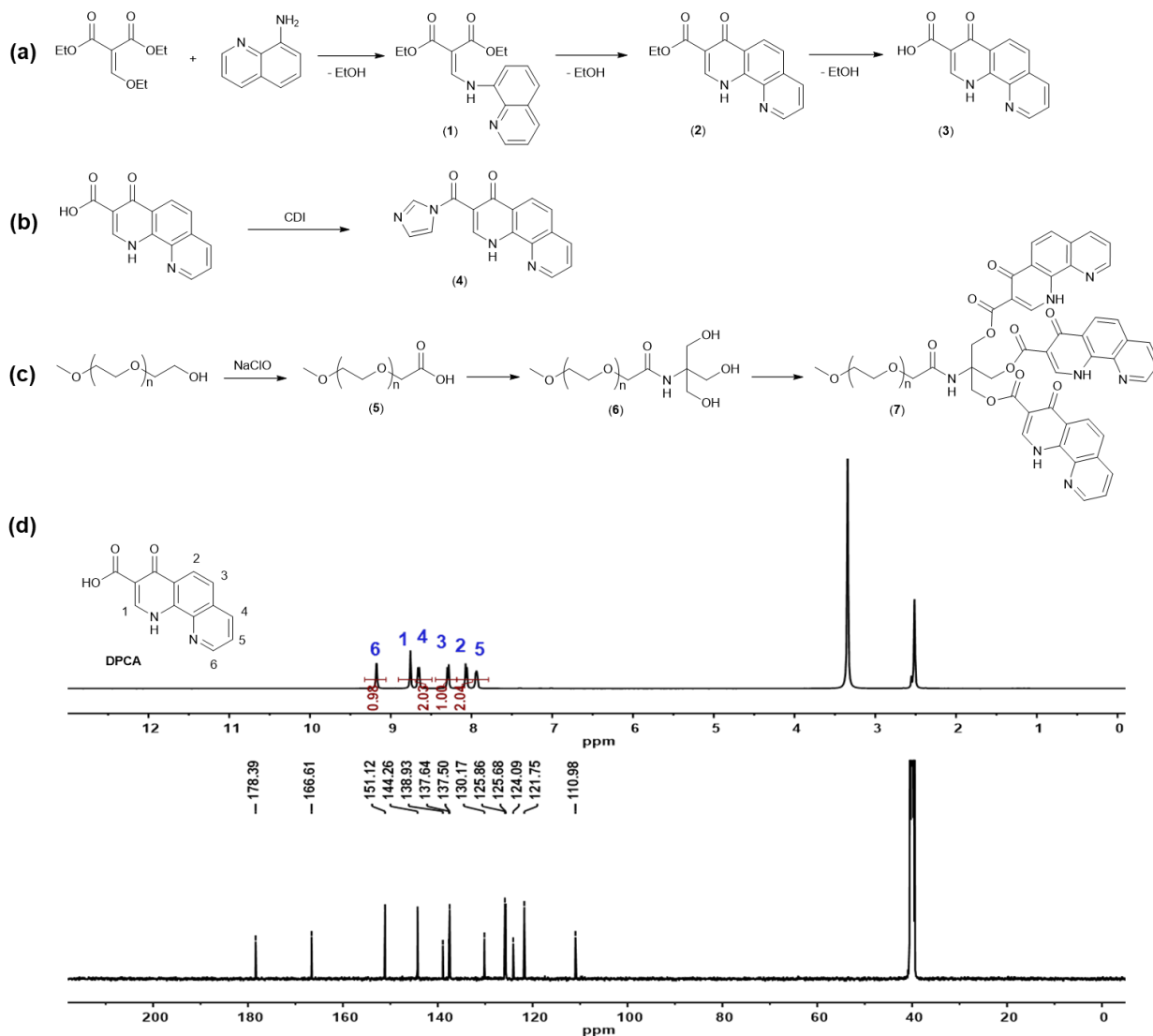


Figure S1. Synthesis of DPCA and PEG-DPCA conjugates(a-c). ^1H NMR and ^{13}C NMR of DPCA in DMSO- d_6 (d).

Synthesis of DPCA-Im (4). DPCA (8 g, 33 mmol) was combined with DMF (150 mL), then added 1,1'-carbonyldiimidazole (16 g, 100 mmol). The mixture was stirred at 100°C for 3 h, and then cooled to room temperature. The product (**4**) was separated by centrifugation and washed with diethyl ether, then dried under vacuum overnight (9 g, 90%).

Synthesis of PEG-triol (6). PEG (10 mmol), TEMPO (0.5 g), NaBr (0.5 g) was dissolved in DI water (400 mL), and NaClO solution (10-15%, 40 mL) was added. pH was adjusted to 10 by NaOH solution (30%), and then the reaction was stirred at RT for 30 min. Ethanol (20 mL) was added to quench the reaction. pH was adjusted to 2 by HCl (10%). The solution was extracted by DCM (100 mL) 4 times. The combined organic solution was then washed with brine, dried by NaSO₄, filtered, and concentrated under vacuum to get product PEG-COOH (**5**). **5** (2 mmol), tromethamine (4 mmol), HBTU (3 mmol) and DIPEA (4 mmol) were dissolved in DMF (10 mL) and stirred at 37°C for 12 h. The product (**6**) was precipitated in diethyl ether (-20°C) and dissolved in DCM (100 mL), washed with 5% HCl three times, washed with brine, dried with NaSO₄, filtered, concentrated under vacuum, precipitated in diethyl ether (-20°C), and dried under vacuum overnight.

Synthesis of PEG-DPCA conjugates. mPEG-OH or PEG-triol (**6**) (1 mmol) was dissolved in 30 mL DMF and NaH (60%, 1.5 eq to hydroxyl group) added. After 10 min DPCA-Im (1 eq to hydroxyl group) was added and the mixture was stirred at 50°C for 30 min to form a clear viscous solution. The product was precipitated in diethyl ether (with 1% acetic acid), washed with methanol/diethyl ether once, then washed with diethyl ether twice, and dried under vacuum overnight (90%, product structures shown in **Figure 1**). Structure characterizations of products **P7D3** and **P80D6** are shown in **Figure S2**.

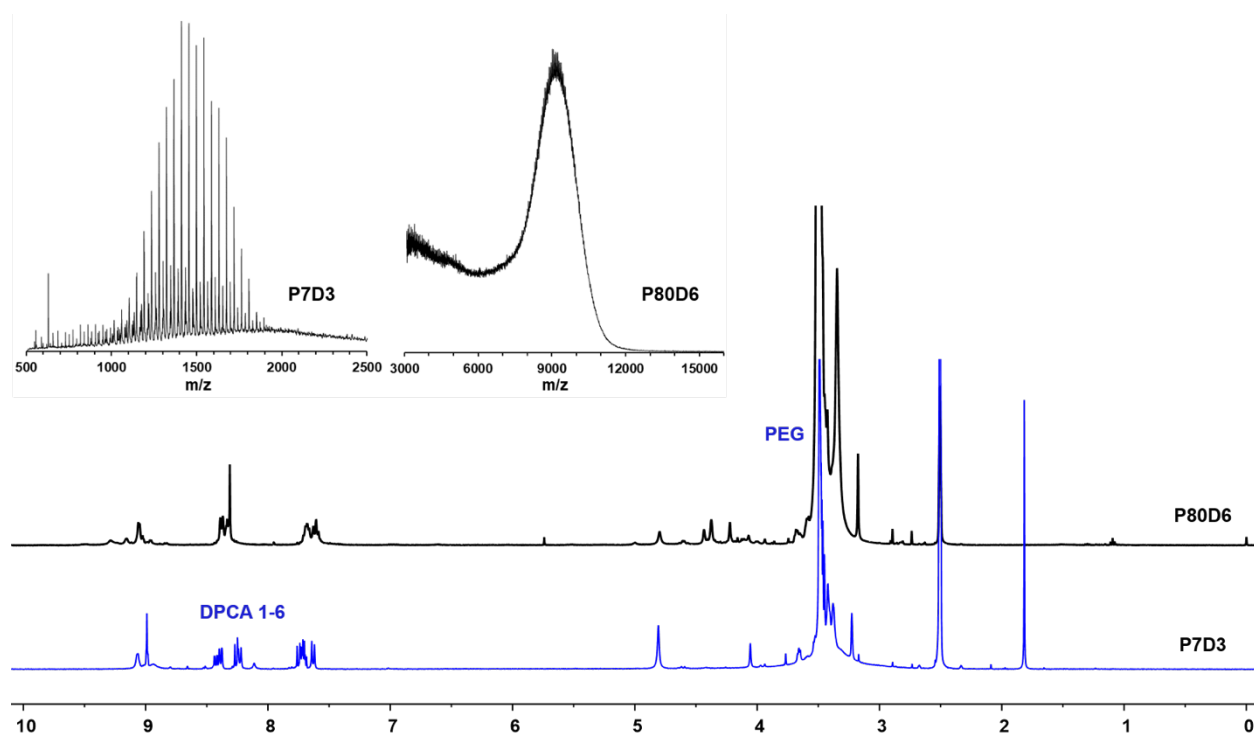


Figure S2. MALDI and ¹H NMR spectra of P7D3 and P80D6.

Preparation and Composition of Supramolecular PEG-DPCA Hydrogels. 100 mg/mL of P7D3 and P80D6 solutions were mixed in different ratios (see **Table S1**). The mixtures were warmed to 50°C and mixed well by vortex for 5 min, then cooled to RT to form a homogeneous hydrogel. Use of a lower molecular weight PEG (4 kDa) for the telechelic bridging polymer resulted in gelation times on the order of hours (data not shown).

Table S1. DPCA content and sol-gel behavior of P7D3 and P80D6 mixtures as a function of composition.

Mixture #	P7D3		P80D6		Wt% DPCA	Liq. or Gel @ 37°C	T _{sol-gel} (°C)
	Mole %	mg/ml	Mole %	mg/ml			
1	100	100	0	0	49.0	L/G	33.5
2	97.5	88.4	2.5	11.6	45.0	L/G	34.5
3	95	75.6	5	24.4	40.8	G	42
4	92.5	66.0	7.5	34.0	37.4	G	44
5	90	58.6	10	41.4	34.9	G	41.5
6	85	47.6	15	52.4	31.2	G	41
7	80	38.5	20	61.5	28.1	G	41
8	75	32.2	25	67.8	25.9	G	45
9	62	20	38	80	21.8	G	50
10	53	15.0	47	85.0	20.1	G	47.8
11	45	11.4	55	88.6	18.9	G	46.5
12	41	10	59	90	18.4	G	46.5
13	35	7.8	65	92.2	17.6	G	46.5
14	25	5.0	75	95.0	16.7	L	*
15	15	2.8	85	97.2	16.0	L	*
16	5	0.8	95	99.2	15.3	L	*
17	0	0	100	100	15.0	L	*

L = liquid; G = gel; * = no transition observed above 10°C

Rheological Study. Rheological characterization was performed on an oscillatory rheometer (MCR-302 modular compact rheometer by Anton Paar) with a parallel plate geometry (25 mm diameter). Dynamic oscillatory strain amplitude sweep and step-strain behavior measurements were conducted at a frequency of 6.28 rad/s and 37°C and 1% or 100% strain applied alternatively. Dynamic oscillatory frequency sweep measurements were conducted at 1% strain amplitude and 37°C. Dynamic temperature-dependent sweep measurements were conducted at a frequency of 6.28 rad/s and 1% strain, with 6°C/min heating and cooling rate. Rheological results of 100 mg/mL mixtures are shown in **Figure S5**, with sample ID correlating to compositions shown in **Table S1**. In **Figure S5d**, samples #18 and #19 were controls in which P7D3 or P80D6 were replaced by

DPCA-free PEG of the same molecular weight, showing the importance of DPCA in the observed rheological behavior.

Dynamic Light Scattering. A Malvern Instruments ZetaSizer Nano ZS (zen3600) was used for DLS study. Diameter and measured Count Rate were calculated from an average of three measurements. Derived Count Rates were obtained by measured count rate divided by the attenuation factor.

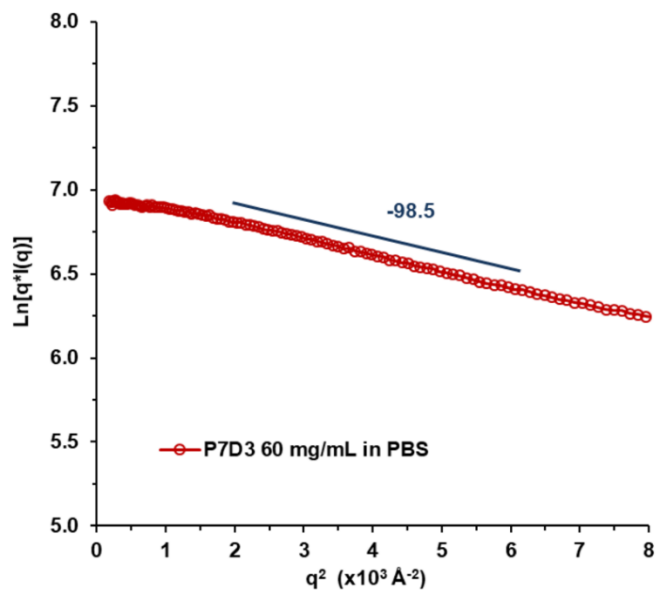


Figure S3. Modified Guinier plot of P7D3 solution.

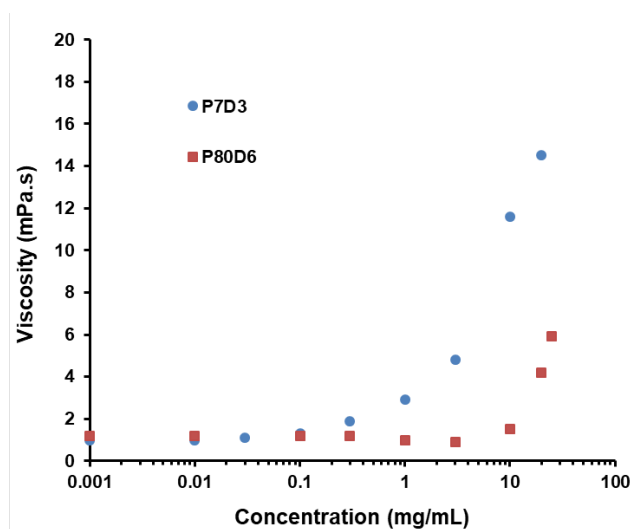


Figure S4. Constant shear viscosity of P7D3 and P80D6 solutions at 20°C.

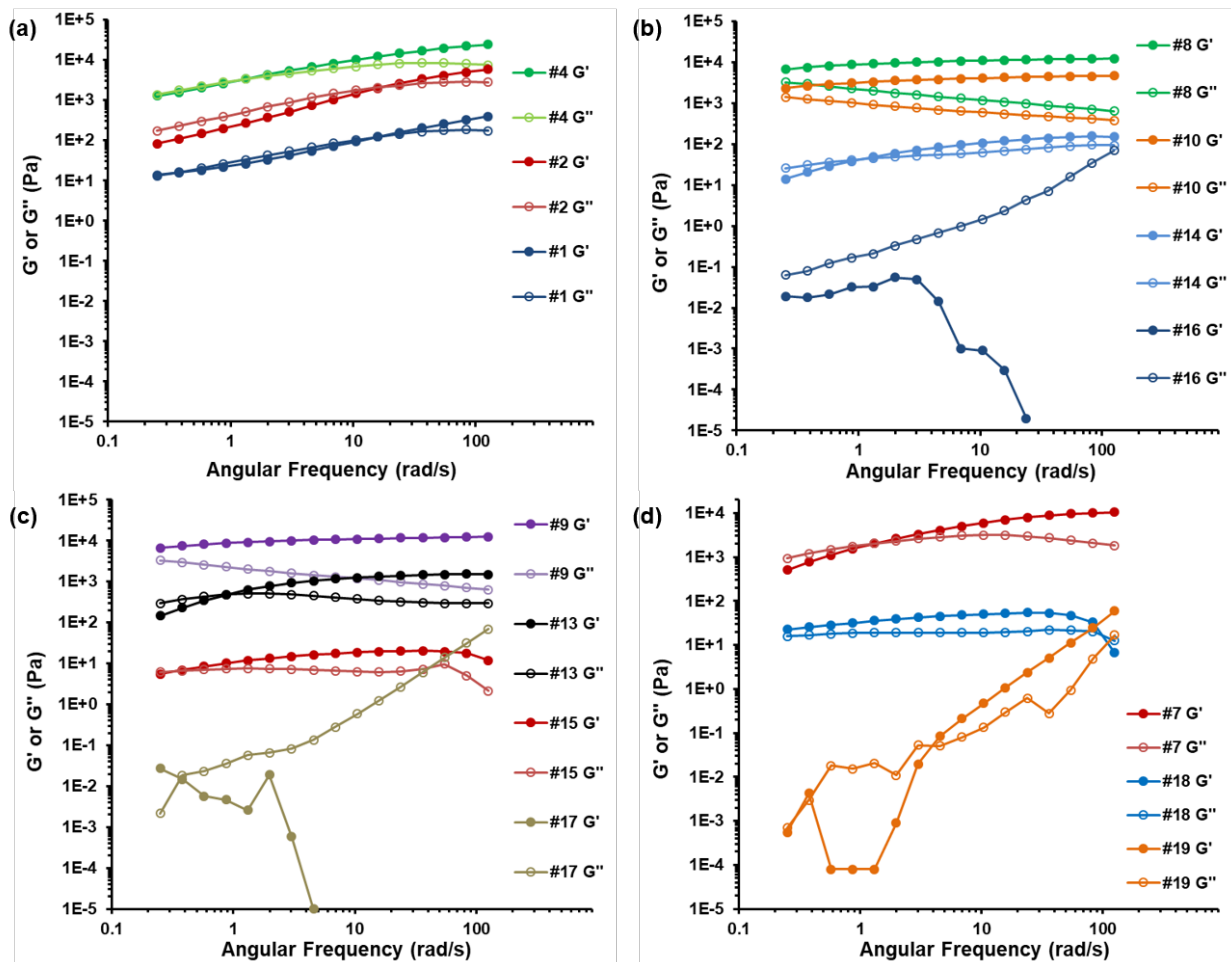


Figure S5. Rheological characterization of P7D3/P80D6 gels. (a)-(d) Frequency sweep study of mixtures #1-#17 shown in Table S1, at 100mg/ml total polymer concentration and $\gamma=1\%$, 37°C . In (d), #18 and #19 are mixtures with same ratio as #7, except that P80D6 was replaced by PEG8k (#18) or P7D3 was replaced by PEG750 (#19).

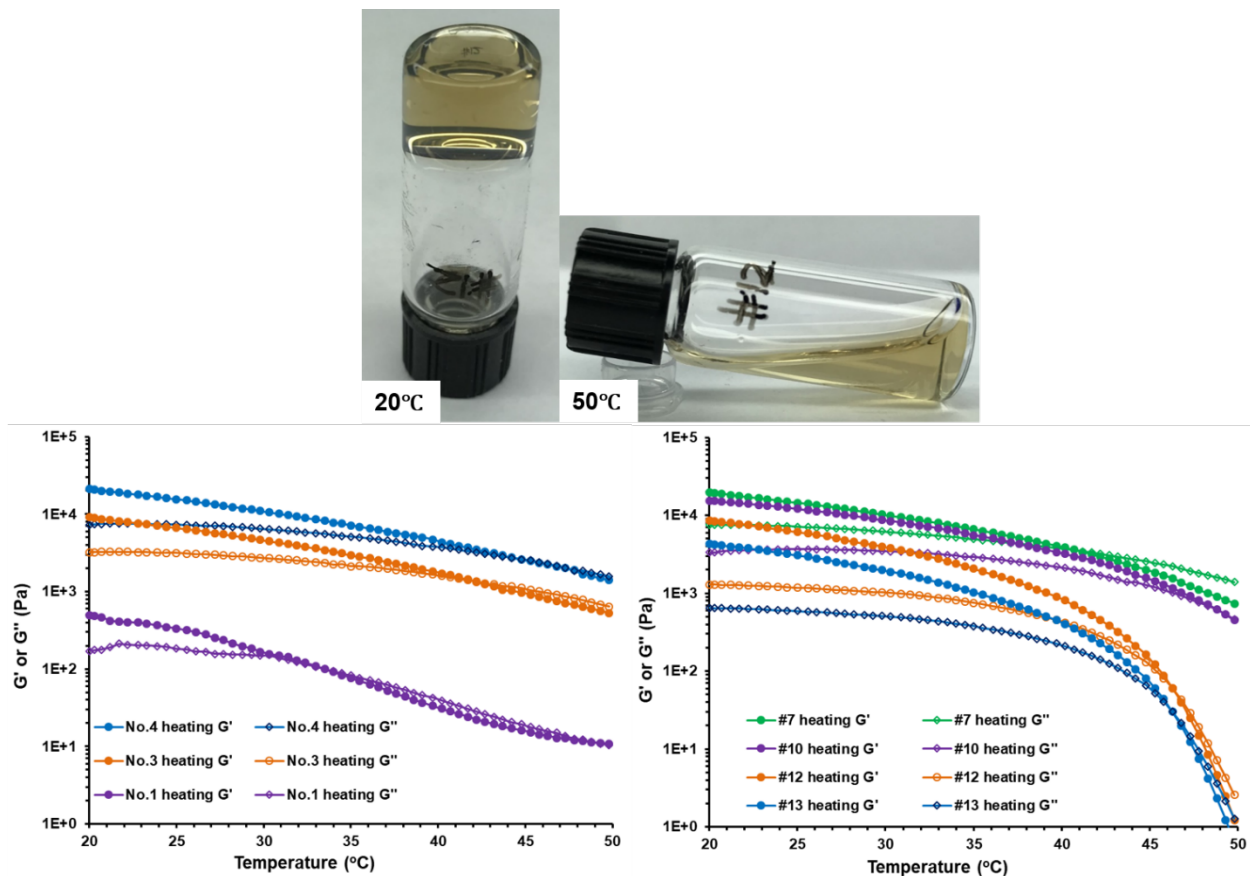


Figure S6. Thermorheological characterization of selected gels ($\gamma=1\%$, $\omega=6.28$ rad/s). The photos at the top show the appearance of gel #12 at 20°C and 50°C.

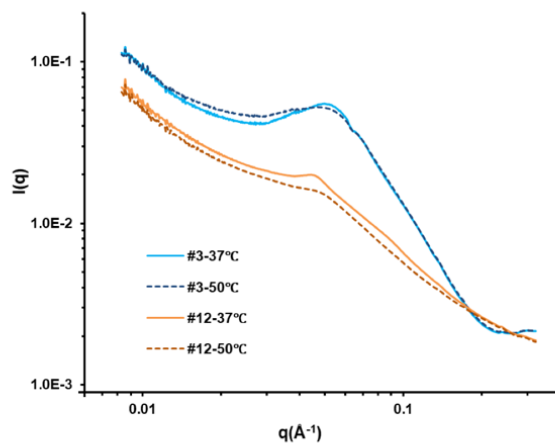


Figure S7. SAXS analysis of P7D3/P80D6 mixtures #3 and #12 at 37° and 50°C.

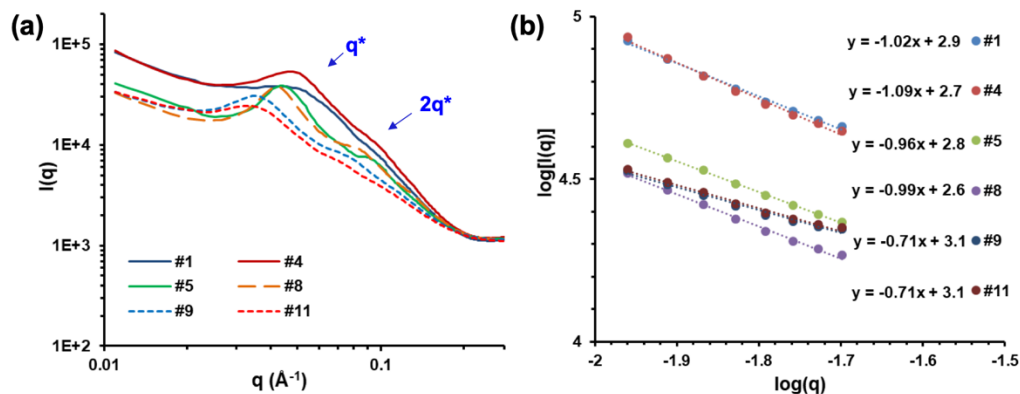


Figure S8. SAXS analysis of P7D3/P80D6 mixtures #1, #4, #5, #8, #9, #11. (a) SAXS patterns at RT; (b) Modified Guinier analysis of the samples, with slope -1 at low q range indicating the presence of cylindrical structures.

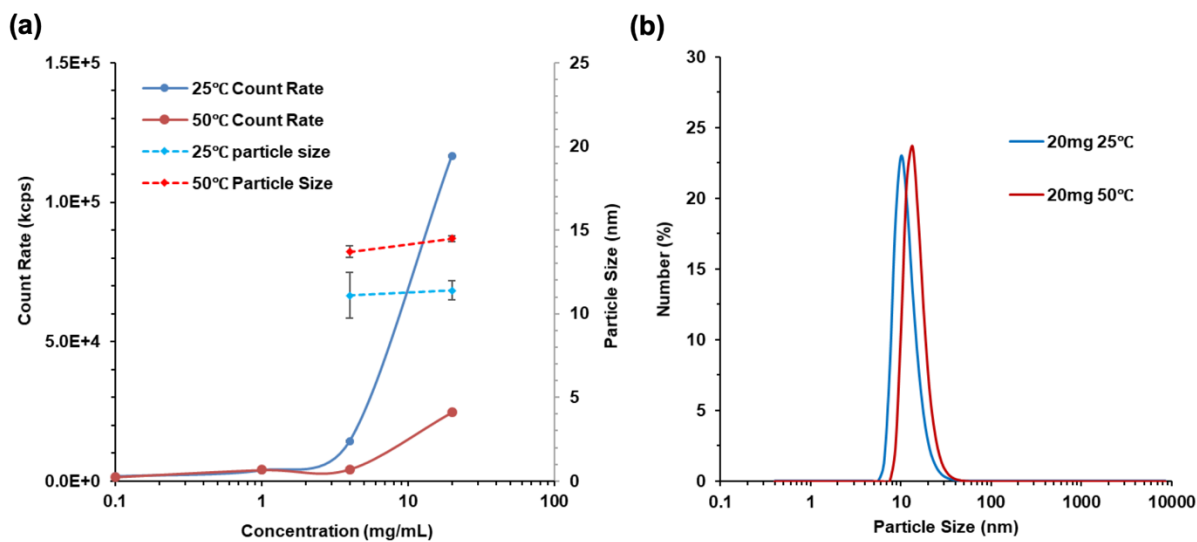


Figure S9. DLS analysis of P80D6 solution. (a) Count rate and average particle size of P80D6 solutions at 25° and 50°C. (b) Particle size distribution by number of P80D6 solution at 25° and 50°C. The decrease of count rate and increase of particle size at 50°C indicated swelling and dissociation of the aggregates while heating.

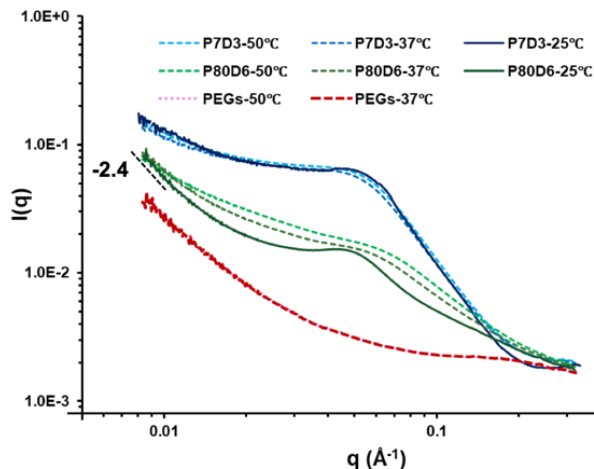


Figure S10. SAXS scattering of P7D3, P80D6 and unmodified PEGs (PEG8k:PEG750 = 9:1, m/m) solution (100 mg/mL) at 25°, 37° and 50°C. The -2.4 slope in the low- q range of the P80D6 scattering curve at 25°C indicated crosslinked nanoparticle network.

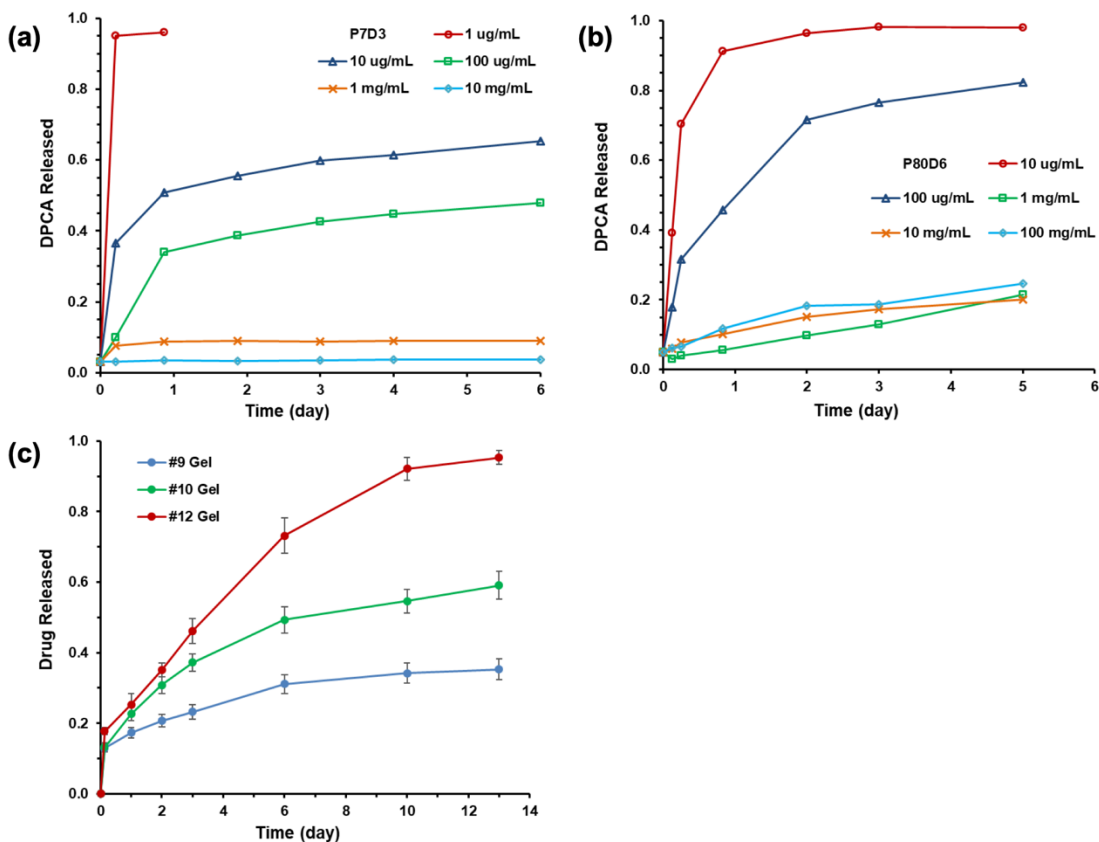


Figure S11. In vitro DPCA release of (a) P7D3 and (b) P80D6 and gel #9, #10 and (c) mixture #12 in PBS buffer at 37°C with shaking (100 rpm).

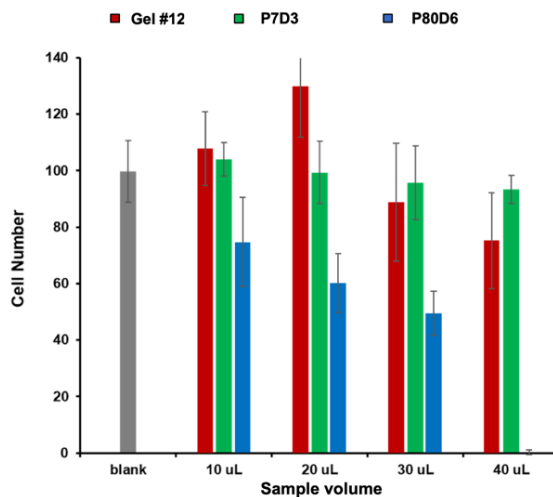


Figure S12. Cytotoxicity of gel #12 toward B6 fibroblast cells.

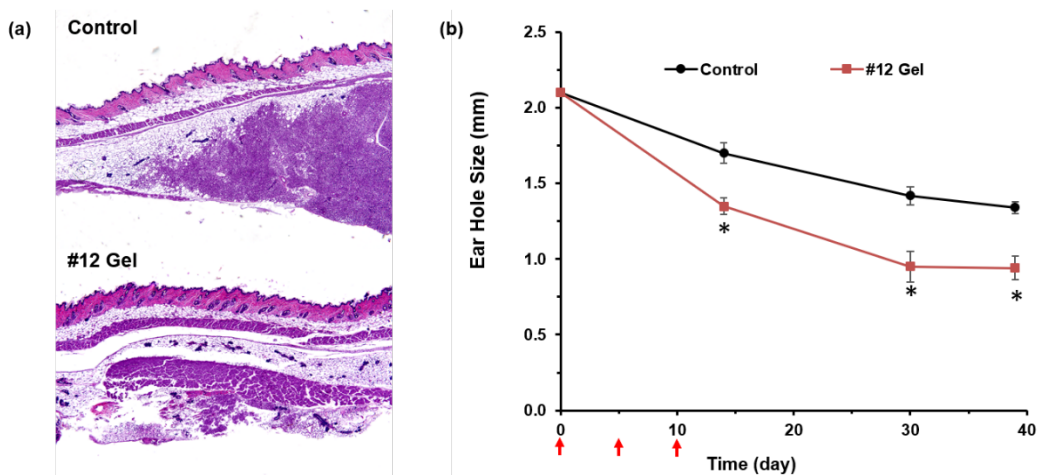


Figure S13. Injection site response and earhole closure for gel #12. (a) Histological sections of the subcutaneous injection site for gel #12 and a PEG control on day 49. (b) Ear hole closure versus time for control and #12 gel treated group. The red arrows indicate time points at which 50 μL of supramolecular gel was administered. ($n = 12$ ears, $p < 0.005$ vs control for all time points)

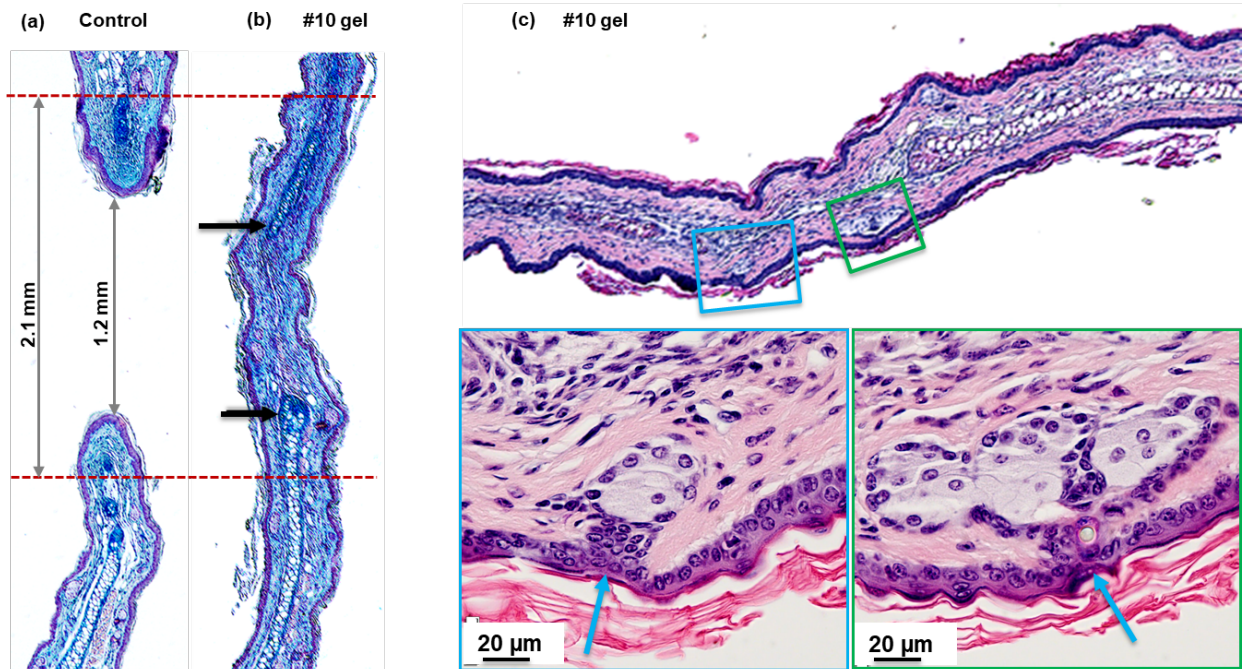


Figure S14. Histological analysis of ear tissue harvested on day 34. The dashed red line indicates the location of the 2.1 mm ear punch. Alcian blue-stained tissue sections from control (a) and #10 gel-treated (b) mice are shown at left. The black arrows in (b) show the margins of the newly regenerated cartilage. Shown in (c) are H&E-stained tissue sections from #10 gel-treated mice. In (c) the two boxed areas and seen 60x magnified below, with the blue arrows indicating new hair follicles within the regenerated region.

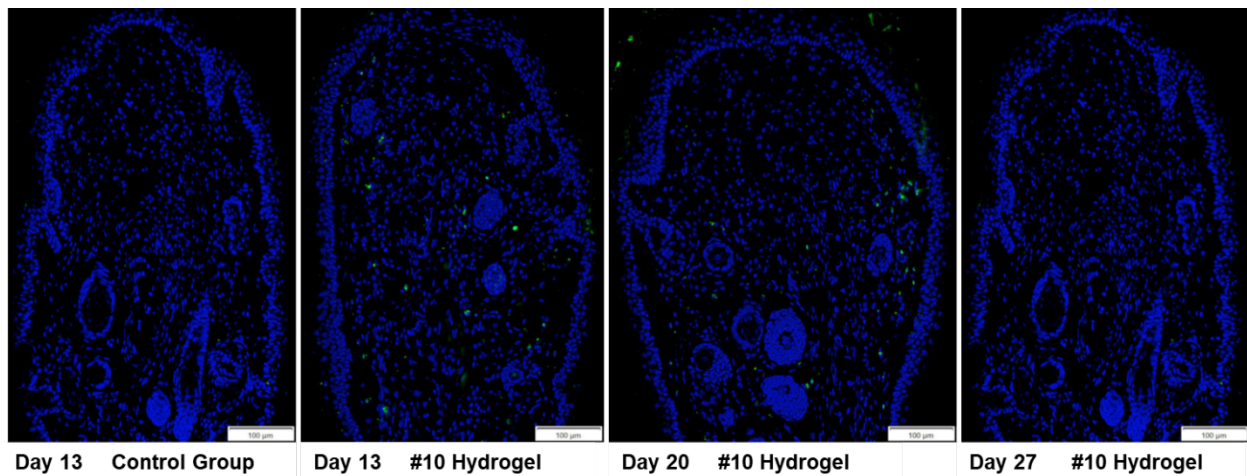


Figure S15. HIF-1 α levels return to normal at 13 days and later in #10 gel treated mice. Female Swiss Webster mice were injected subcutaneously with 25 μ L of gel #10 on days 0, and 8 after ear hole punching, with no injection for the control group. Ear tissue was harvested on days 13, 20, and 27 for HIF-1 α immunostaining (green). Little or no staining was seen at these timepoints compared to the intense staining seen at earlier time points, supporting the notion that we achieved a biphasic HIF-1 α response similar to that seen in the MRL mouse during the regenerative response.^{1,2}

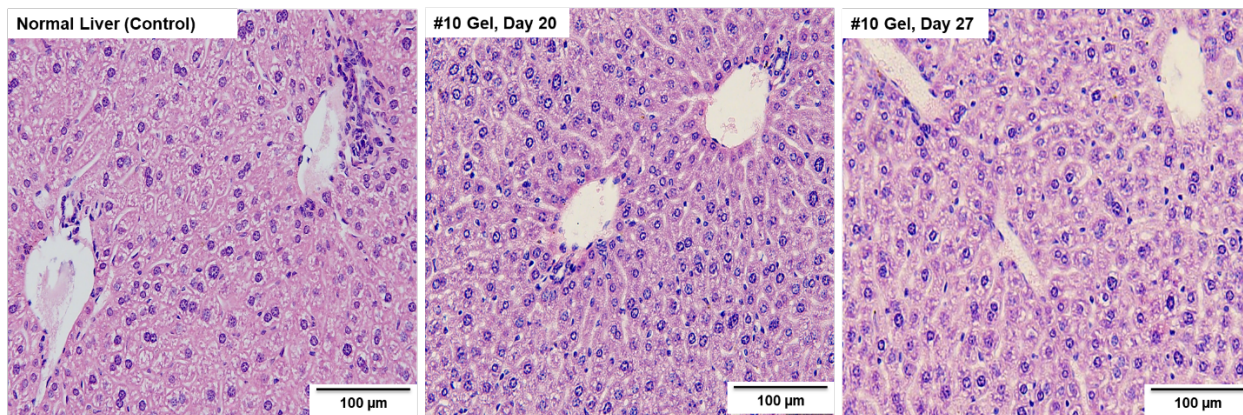


Figure S16. H&E stained histological sections of liver tissue taken on day 20 and 27. Female Swiss Webster mice were injected subcutaneously with 25 μL of gel #10 on days 0, and 8 after ear hole punching. There is no evidence of pathology, cell invasion, inflammation, or obvious toxicity as a result of drug administration compared to normal liver. Normal liver (Control) was taken from untreated mice.



Figure S17. Discoloration of skin at injection sites of PEG control group, indicating the formation of hematomas as confirmed by histology seen in S13a.

Table S2. Antibodies used for Immunostaining.

	Primary antibody			Secondary antibody		
	Company	Cat. No.	Dilution	Company	Cat. No.	Dilution
HIF-1 α	Abcam	ab2185	1:200	Molecular Probes	A11008	1:300
NANOG	Santa Cruz Biotechnology	sc-33760	1:150	Molecular Probes	A11036	1:300
Oct-3/4	Santa Cruz Biotechnology	sc-5279	1:150	Molecular Probes	A11061	1:300
CD133	Emd Millipore	MAB4310XMI	1:150	Molecular Probes	A11007	1:300
CD34	Bioss Inc.	bs-0646R	1:150	Molecular Probes	A11007	1:300
PAX7	R&D Systems	MAB1675	1:50	Molecular Probes	A11061	1:300
PREF-1	Novus Biologicals	NBP237548	1:150	Molecular Probes	A11007	1:300
NESTIN	Thermo Scientific	PIMA1110	1:150	Molecular Probes	A11005	1:300
vWF	Thermo Scientific	PA516634	1:50	Molecular Probes	A11008	1:300

References

1. Zhang, Y.; Strehin, I.; Bedebaeva, K.; Gourevitch, D.; Clark, L.; Leferovich, J.; Messersmith, P. B.; Heber-Katz, E., Drug-Induced Regeneration in Adult Mice. *Sci. Transl. Med.* **2015**, *7*, 290ra92.
2. Heber-Katz, E., Oxygen, Metabolism, and Regeneration: Lessons from Mice. *Trends Mol. Med.* **2017**, *23*, 1024-1036.